JOURNAL OF MATERIALS SCIENCE 10 (1975) 551–562

Carbon fibre composites with rubber toughened matrices

J. M. SCOTT, D. C. PHILLIPS
Process Technology Division, AERE, Harwell, Didcot, Oxon, UK

In carbon fibre reinforced plastics (CFRP), the initial resistance to crack propagation parallel to fibres is determined largely by the matrix toughness. The fracture toughness (G_{IC}) of an epoxide resin can be increased considerably by the addition of butadiene-acrylonitrile co-polymers (CTBN). These cause the precipitation of small spheres of a second phase and, for example, increase G_{IC} from $\sim$ 300 to $\sim$ 3000 J m^{-2} on the addition of 9 wt% CTBN. The large increases obtained in bulk resins are not obtained in CFRP, instead significant but modest increases are achieved. The suppression of toughness is related to the thickness of resin film through which the crack propagates.

1. Introduction

In the development of fibre composites, most attention has been concentrated on the behaviour of the material under stresses in the fibre directions. This behaviour is dominated by the properties of the fibres, and in carbon fibre reinforced plastics (CFRP) the properties of the matrices tend to be regarded as of relatively minor importance. An example of fibre dominated behaviour is the tensile fatigue of unidirectional CFRP in which the excellent tensile fatigue behaviour of the fibres results in good tensile fatigue behaviour of the composite.

In many practical uses of CFRP, however, situations can occur in which dangerously high stresses may arise in the matrix and result in crack propagation parallel to the fibres in the matrix or fibre-matrix interface. Examples of matrix dominated behaviour are the rapid degradation which can occur during shear fatigue [1], and ballistic impact damage due to the occurrence of high transient shear or transverse tensile stresses [2]. In such situations the resistance of the composite to crack propagation parallel to the fibres is of considerable importance.

Like other composite properties, the resistance to crack propagation is highly anisotropic. For cracks propagating perpendicularly to fibres, fracture energy (G_c) values are obtained ranging from a few kJ m^{-2} for high modulus surface-treated fibres to a few tens kJ m^{-2} for surface-untreated and high strength surface-treated fibres [3, 4]. In an ideal, perfectly aligned composite it seems probable that the resistance to crack propagation in a direction parallel to fibres would be approximately equal to the resistance of the matrix material. Typically this is $\sim$ 0.15 kJ m^{-2} for a DGEBA epoxide resin – a type commonly used for composites. In reality, because the fibres in CFRP are not perfectly aligned, there can be a contribution to G_c from the misaligned fibres through processes characteristic of a composite, such as pull-out or debonding, occurring in and around a tied zone at the crack tip. A tied zone is a region in which the crack has propagated through the matrix, but the opposite faces are still held together by fibres which are unbroken, or are broken but not pulled out. Experimentally it has been found [2] that a sharp crack may be introduced into a composite with a tied zone which is initially very small. When the crack is caused to extend, the tied zone can increase in length until it reaches some size determined by the fibre misalignment. Thus the fracture energy G_c may increase from a value similar to that of the matrix material to a much greater value as the crack propagates. This effect makes the definition and reproducible measurement of toughness more difficult than for a homogeneous material. In cross-laminated materials cracks can propagate entirely in resin in the laminate plane without producing a tied zone.

Since at least the initial growth of a crack in a direction parallel to the fibres is controlled by the toughness of the matrix, the use of tougher resins would be expected to lead to an improve-

ment in the matrix dominated properties controlled by this failure mode. The toughness of epoxide resins can be enhanced by the addition of certain butadiene-acrylonitrile co-polymers (CTBN) which precipitate in the resin as small spheres during curing [5]. This rubber precipitation process possesses advantages over other toughening mechanisms such as by the addition of a dissolved flexibilizer, as it results in toughening with relatively small decreases in resin rigidity, or glass transition temperature [6]. There have been several studies of the effect of the addition of CTBN on the fibre dominated properties of reinforced plastics. In GRP it has been shown to result in reduced crack densities in the matrix during tensile fatigue and an improvement of fatigue life [5]. In CFRP, matrix cracking under tensile stressing is not a significant effect and no significant improvements have been observed in fibre dominated properties [7, 8]. This paper describes the results of a study of the effect of rubber particle precipitation on cracks propagating parallel to fibres in CFRP – a matrix dominated behaviour. It also describes the flexural properties of rubber toughened CFRP and shows that the addition of CTBN does not degrade these conventional properties at ambient temperatures. During the study, it was observed that the toughness of the toughened resins was greatly suppressed when the material was constrained into a thin film. An account, therefore, is included of crack propagation through thin adhesive layers.

2. Materials and specimen preparation

The epoxide resin used throughout was Ciba-Geigy MY750. This is an unplasticized diglycidyl ether of bisphenol A (DGEBA) with a mean molecular weight of about 300 and an epoxide equivalent of 5.0 equiv kg^{-1}. Three samples of liquid carboxyl terminated butadiene-acrylonitrile co-polymers (CTBN) with varied acrylonitrile contents were supplied by the B. F. Goodrich Chemical Company. A fourth, older sample had been acquired some time previously and was included in the study although less was known about its properties. The Goodrich company has observed that in a similar epoxide system to MY750 the rubber particle size decreases with increasing acrylonitrile content, so that with these samples a range of sizes could be obtained. Table I shows details of the CTBN rubbers.

TABLE I The CTBN polymers

Polymer	Acrylonitrile content (%)	EPHR*
A	Unknown	Unknown
B	24.2	0.054
C	28.0	0.047
D	18.0	0.054

*EPHR = equivalent per hundred parts of rubber.

The rubber toughened epoxide was produced in batches by mixing 100 g MY750 with the required weight of CTBN and then adding 6 g piperidine as a curing agent. It is common practice to degas a liquid epoxide system by placing it in a vacuum chamber before curing in order to prevent the entrapment of air bubbles. It was found that this procedure was not suitable for degassing a CTBN:MY750:piperidine mixture as it resulted in prolonged foaming. Instead, the mixture was warmed to reduce its viscosity and then after a few minutes either cast into a vertical mould 20 cm × 15 cm × 0.6 cm to produce a resin plate, or else used to manufacture composites. Few bubbles were apparent to the naked eye in the cast resin plates.

The rubber toughened resins and their composites have been compared with the untoughened resins and their composites. The untoughened resin systems were 100 parts by weight (p.b.w.) MY750 + 6 p.b.w. piperidine, and 100 p.b.w. MY750 + 80 p.b.w. methyl nadic anhydride (MNA) + 1 p.b.w. benzyldimethylamine (BDMA). The latter is a common system used to manufacture CFRP. These systems were degassed in the normal manner.

Composites were produced by a wet lay-up technique in the form of unidirectional bars 30 cm × 2.5 cm × 0.6 cm and 30 cm × 1.25 cm × 0.25 cm. The required quantity of fibres to make a 60 vol % composite was first soaked in warm resin, then gently squeezed to remove excess resin, and finally placed in a mould and pressed to stops.

Adhesive films were produced by sandwiching the resin between aluminium alloy adherends. The aluminium adherend surfaces were prepared by immersion for 20 min at 61 °C in a solution of 1600 ml water, 300 ml concentrated sulphuric acid and 100 g chromium trioxide; followed by washing in water and drying at 62 °C. These temperatures have been recommended [9] to avoid a change in the alumina phase at 67 °C. The dry, prepared surfaces were then coated with the viscous, liquid resin and held together

by clamps, the glue-line thickness, of 0.1 or 0.2 mm, being determined by metal spacers.

When piperidine was used as the curing agent, the cast resin, adhesive and composites were cured for 16 h at 120°C. The MY750:MNA:BDMA systems were cured for 2 h at 120°C.

3. Test methods

Fracture energies were determined by double cantilever beam (DCB) techniques for cracks propagating in bulk cast resin; along thin adhesive films of resin; and parallel to the fibres in CFRP. Different specimen geometries were used for the three types of measurement and two of these are shown in Fig. 1.

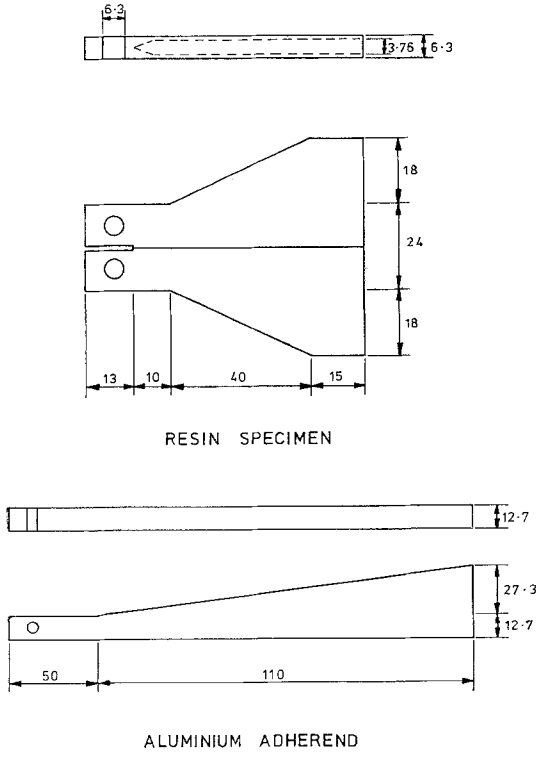

Figure 1 Tapered DCB specimens. Dimensions in mm.

The fracture energy (G_c) of a material, a measure of its resistance to crack propagation, is related to the load (P) required to propagate the crack and the variation of specimen compliance C with crack area A by

$$G_c = \frac{P^2}{2}\frac{\partial C}{\partial A}. \quad (1)$$

The tapered DCB specimens shown in Fig. 1 and used for the bulk epoxide and adhesive films, are shaped so that $\partial C/\partial A$ remains constant with increasing crack length [10]. Provided G_c remains constant, crack propagation occurs under constant load. It can be shown that for a tapered DCB specimen of an elastically isotropic material

$$G_c = \frac{4P^2m}{b\,b'E} \quad (2)$$

where b is specimen thickness, b' is crack plane width, E is Young's modulus and m is a constant which depends only on the specimen shape. Experimentally, the procedure consists of determining m for the specimen geometry by measuring the variation of compliance with crack length, (Fig. 2). G_c may then be obtained from a similar specimen of any other isotropic material from the load which causes the crack to propagate, and the material's Young's modulus. For the bulk epoxide the compliance calibration was effected by simulating cracks by saw cuts made by a fine jeweller's saw, and Young's modulus was measured by three-point bend tests. For the adhesive joints, crack propagation occurred in a characteristic stick-slip manner. The positions of the crack arrests were clearly and accurately marked on the fracture surfaces by crack arrest lines, and these provided sufficient information to enable a compliance calibration.

For ease of fabrication, a parallel sided DCB specimen was used to measure the fracture energies of the composites. Because of the material anisotropy side-grooves were unnecessary to guide the cracks. Six DCB CFRP specimens were made from each resin composition. From each set, two were selected and the compliance measured as a function of crack length for saw-cut cracks as shown in Fig. 3. Fracture energies were then obtained from the remaining two specimens through Equation 1. This was accomplished by introducing a crack with a jeweller's saw and sharpening it by pressing a razor blade into the crack tip; loading the specimen to cause the crack to propagate a short distance; unloading the specimen to obtain its compliance; relating the compliance through the compliance calibration to $\partial C/\partial A$; and reloading the specimen to obtain the load at which the crack propagated again. Fig. 4 shows the typical load versus displacement curve for such an exercise. During crack propagation a tied zone was created, as described in the

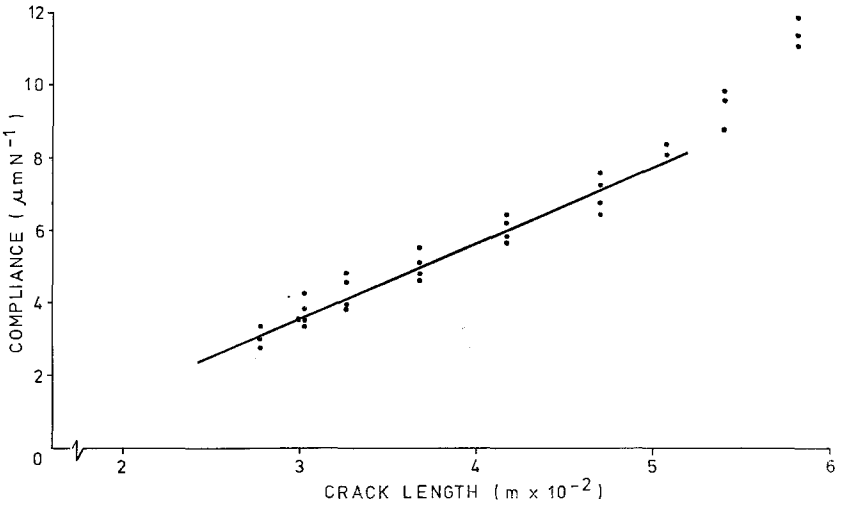

Figure 2 The variation of compliance with crack length of a tapered DCB.

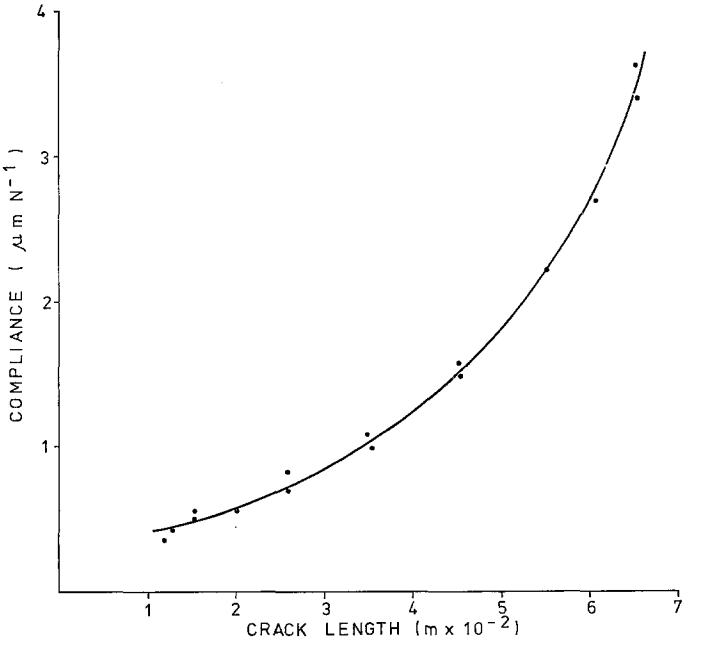

Figure 3 The variation of compliance with crack length of a parallel sided DCB.

Introduction, and the calculated fracture energies varied with crack length. Because the method of obtaining the compliance calibration used a saw-cut as a simulation of a crack, and thus did not take into account the effect of a tied zone on the compliance, the accuracy of the fracture energy measurements decreased as the crack grew.

All fracture energy measurements were carried out in an Instron testing machine at a cross-head speed of 0.5 mm min^{-1}. The flexural strengths, interlaminar shear strengths and flexural moduli

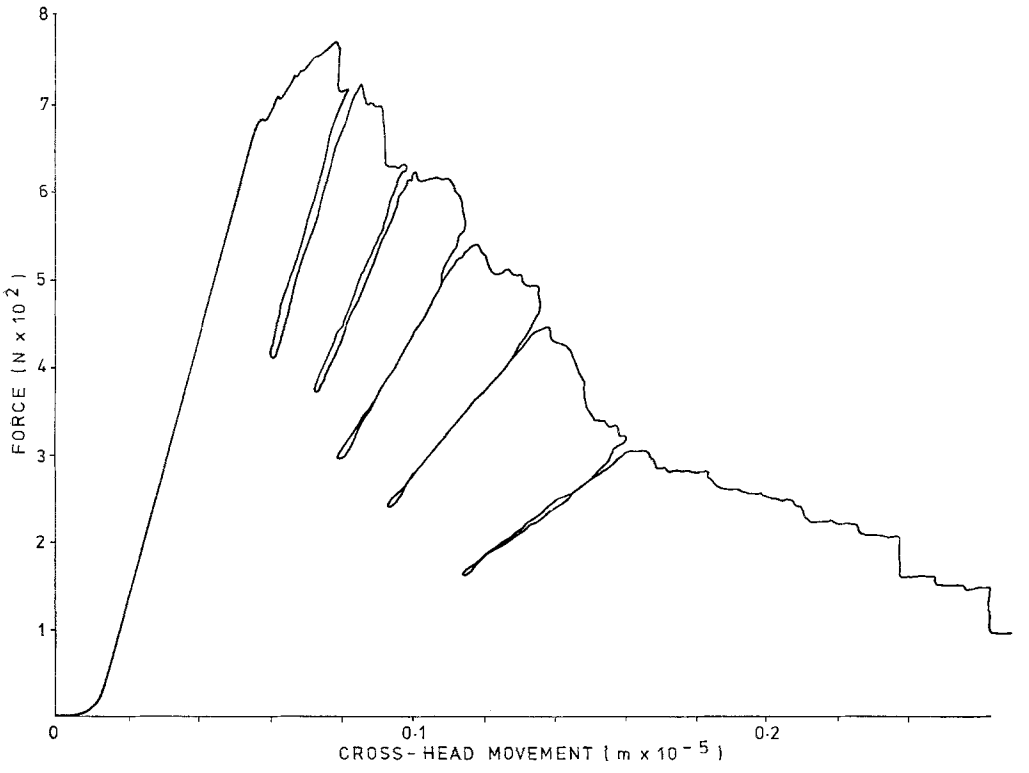

Figure 4 The load-displacement curve of a CFRP, DCB specimen.

of the composites were determined by three-point bending. Span to depth ratios were respectively 16:1, 5:1 and 100:1, and the specimen cross-sections were 12.5 mm wide × 2.5 mm deep.

Some compressive yield measurements also were made on the unreinforced resins. These specimens consisted of small, cast cylinders 10 mm in diameter and 20 mm high and were compressed at a cross-head speed of 0.5 mm min^{-1}.

4. Results and discussion

4.1. Toughening of the bulk resin

Fig. 5 shows the variation of resin toughness with concentration of CTBN. Each point is the mean of several measurements made on each of three DCB specimens of a given composition. Since all three were obtained from a single plate, the detailed variation of G_c with CTBN content may not be accurate. However, there is a clear trend of G_c tending to increase with CTBN concentration. The maximum mean value of 3.16 kJ m^{-2} is an order of magnitude greater than the values measured for the untoughened resins, which were 0.33 $\pm$ 0.2 kJ m^{-2} for the piperidine cured MY750 and 0.16 $\pm$ 0.01 kJ m^{-2} for the MY750:MNA:BDMA system. Table II shows the variation with CTBN concentration of Young's modulus, which has been determined to an accuracy of $\pm$ 3%. There is a tendency for a decrease in stiffness with increased CTBN.

TABLE II The dependence of Young's modulus (GN m^{-2}) of the resin on CTBN concentration

Polymer concentration (wt%)	Polymer type			
	A	B	C	D
3.2	2.9	2.9	2.9	2.7
6.2	3.1	2.3	2.7	2.7
9.0	2.6	2.4	2.4	2.5

MY750 + 6% piperidine, 2.9 GN m^{-2}.
MY750/MNA/BDMA 3.6 GN m^{-2}.

Two types of fracture behaviour were observed. In some specimens the crack propagated continuously at a speed determined by the Instron cross-head, which resulted in a load versus deflection (or time) curve of the form shown in Fig. 6a. In other specimens the crack

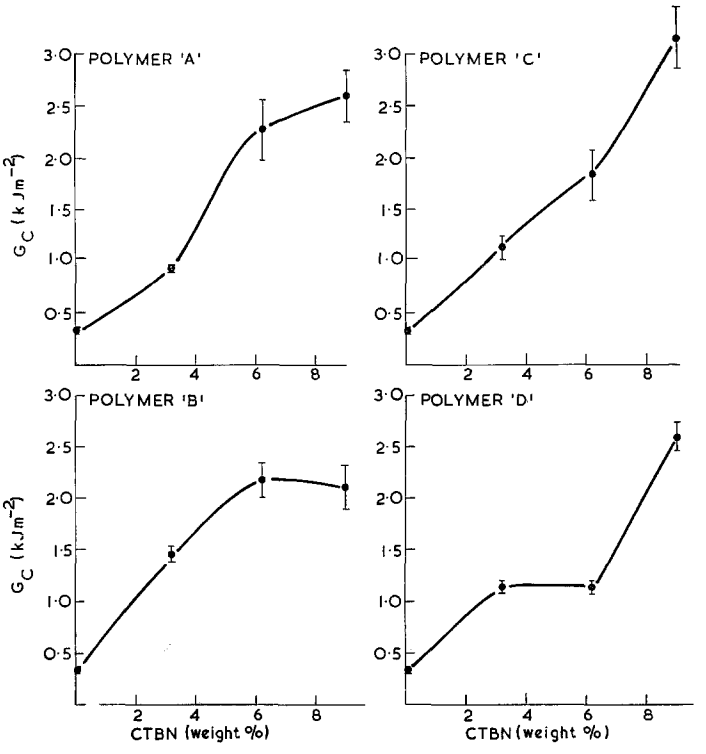

Figure 5 The effect of CTBN concentration on resin fracture energy.

intermittently moved rapidly (stick-slip) at a speed which was independent of the cross-head speed, resulting in a curve as shown in Fig. 6b. These two effects sometimes occurred in apparently identical materials. By far the majority of specimens of all types displayed stick-slip behaviour, with peak loads about 50% higher than trough loads. Where stick-slip behaviour occurs it is possible to define two fracture energies. A so-called initiation energy corresponding to the peak load, and a so-called arrest energy corresponding to the trough load. In this paper only the initiation energies are reported.

During stick-slip behaviour, it has been shown by ciné photography and other observations not reported here, that the crack propagates rapidly causing a smooth surface and then slows down causing a rough region, finally arresting close to the start of the next smooth region. Fig. 7 shows these features on the surface of an untoughened resin. The rubber toughened resins displayed rougher fracture surfaces and Fig. 8 is a high magnification optical micrograph of the equivalent of the smooth region. Whereas in an untoughened resin at that magnification the micrograph shows no features, there is a great deal of detail on the toughened resin fracture surface. Precipitated rubber particles can be seen in Fig. 8, and Fig. 9 is a high magnification scanning electron micrograph of a gold-coated fracture surface showing a rubber particle in more detail.

Fig. 10 is an optical micrograph of a polished rubber toughened resin specimen. From such photographs, and SEM photographs of fracture surfaces, the sizes and numbers of particles have been estimated roughly. Because the rubber spheres are distributed randomly in the matrix, a polished plane will show a range of circle diameters even if all the particles are of the same size. The particles are not all the same size and in order to compare the different materials Table III shows the number of circles in 100 μm^2 and the diameter of a few of the largest of each. The table shows the results obtained both by optical microscopy of polished sections (P) and scanning electron microscopy of fracture surfaces (F).

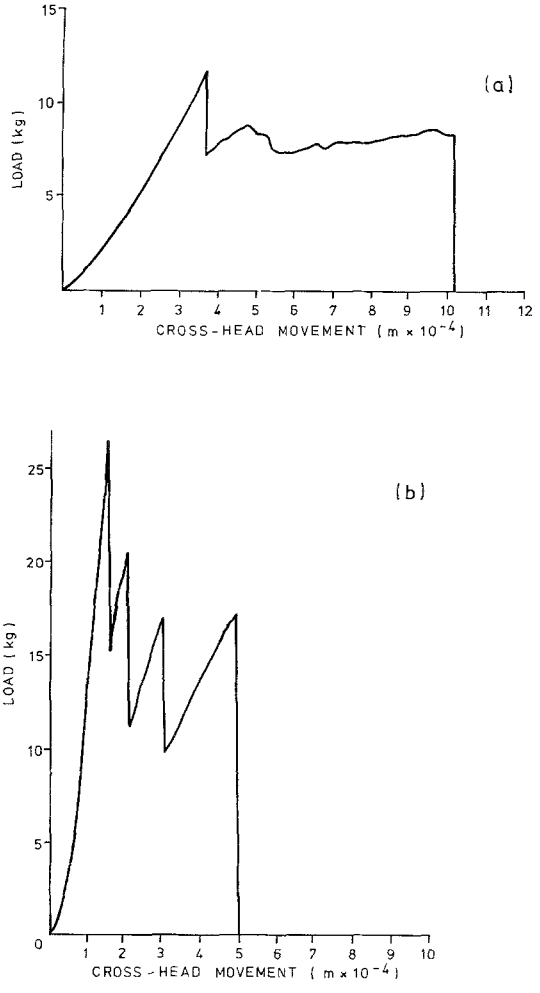

Figure 6 (a) Load-displacement behaviour of continuous crack propagation. (b) Load-displacement behaviour of stick-slip propagation.

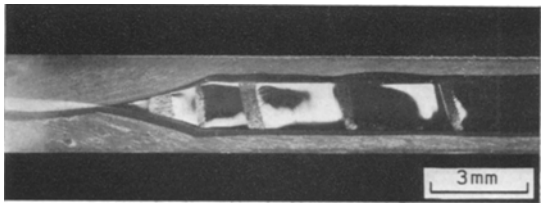

Figure 7 Fracture surface of a resin after stick-slip propagation.

4.2. Rubber toughened CFRP

Three different compositions of rubber toughened resin were used to manufacture composites. They consisted of 9 wt % polymer C, and 3.2 and 6.2 wt % polymer B, thus representing three different sphere sizes. They were compared with composites of MY750:MNA:BDMA and MY750:piperidine.

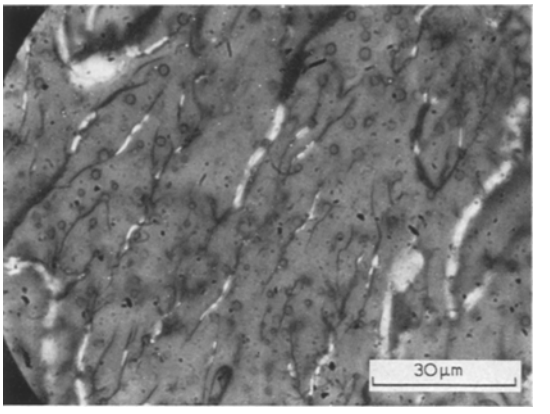

Figure 8 Fracture surface of a rubber toughened resin.

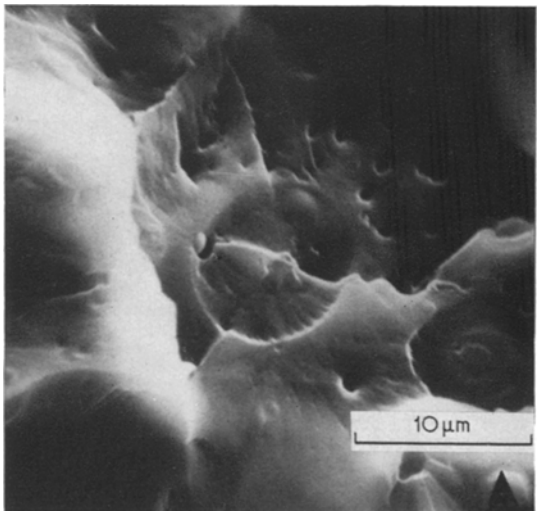

Figure 9 Scanning electron micrograph of a rubber precipitate.

The same carbon fibre tow was used to make all the composites. Because the strength and modulus of carbon fibres sometimes vary along the tow, these properties were measured by single filament tests on samples of tow taken immediately before and after the length used to make each specimen. Table IV shows this information for the fibres and Table V shows the mean values of flexural strength, flexural modulus and interlaminar shear strength measured from each composite and normalized to 60 vol %. There are little or no significant differences in these conventional flexural pro-

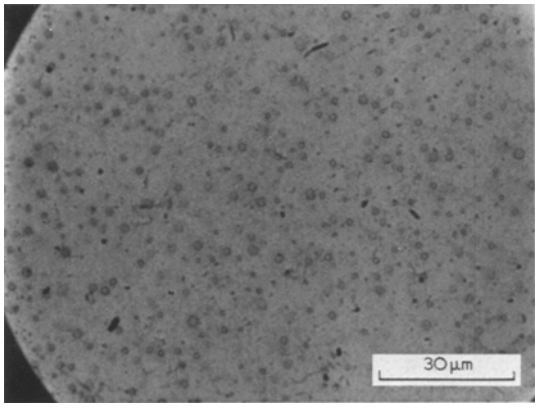

Figure 10 Polished section of a rubber toughened resin.

TABLE III Microstructure of rubber toughened resins P refers to polished sections, F to fracture surfaces.

(a) Largest particle diameter* (μm)

Polymer type	Polymer concentration (wt%)		
	3.2	6.2	9.0
A (P)	1.0	1.9	2.2
(F)	1.2	2.1	2.9
B (P)	0.6	1.2	1.5
(F)	0.8	1.1	
C (P)	0.5	0.5	1.5
(F)	0.8	0.9	1.6
D (P)	1.3	1.2	4.5
(F)	1.3	1.5	4.0

*Obtained by measuring a few of the largest.

(b) Number of particles (all sizes) in 100 μm²

Polymer type	Polymer concentration (wt%)		
	3.2	6.2	9.0
A (P)	9.5	5.5	6.3
(F)	10.7	15.9	4.9
B (P)	7.8	8.3	5.0
(F)	19.0	24.0	
C (P)	8.0	12.0	6.0
(F)	12.0	31.0	19.0
D (P)	7.5	7.0	1.3
(F)	6.0	13.0	4.3

perties between the composites at ambient temperatures.

Toughness data obtained from the composites are shown in Table VI and Fig. 11. Table VI shows the mean initial fracture energies calculated from the observed loads at which a sharpened saw-cut crack began to grow, before the development of a tied zone. These were

TABLE IV Carbon fibre data. Mean values of tensile strength and Young's modulus. Uncertainties are: strength 3%; modulus 1%

Sample	Property	
	Strength (MN m^{-2})	Young's modulus (GN m^{-2})
Before C1	3020	424
Between C1 and C2	2961	431
Between C2 and C3	2951	419
Between C3 and C4	2829	417
Between C4 and C5	2930	405
After C5	3182	404

obtained by making one or more measurements on each of at least two specimens each of two separate composite bars of a given composition. Each mean value is the average of between six and nine measurements. Fig. 11 shows the typical increase in required fracture energy as a sharpened saw-cut crack grew and developed a tied zone. The data were obtained from one specimen containing 6.2% polymer B. Here G_c is plotted against an effective crack length obtained from the compliance calibration and, for reasons outlined in Section 3, the calculated fracture energy and crack length become less accurate as the tied zone grows. However, the increase of required fracture energy with increasing tied zone is clear. The microstructure of the rubber toughened composite is shown in Fig. 12, which is an optical micrograph of a polished section. The presence of precipitated rubber spheres in the matrix can be seen clearly.

From Table VI, it can be seen that the initial fracture energies obtained from composites of untoughened resin are very similar to the fracture energies of the resins themselves. However, the initial fracture energies obtained from the composites of toughened resin are considerably lower than those of the resins alone, and display only very modest increases in toughness over those of the untoughened resin composites. The similarity between the interlaminar shear strengths of the toughened and untoughened composites suggests that the fibre-matrix interface is not significantly weakened by the presence of CTBN. The micrograph (Fig. 12), shows that the presence of fibres does not prevent the precipitation of rubber spheres. Therefore, clearly some mechanism is suppressing the toughening effect

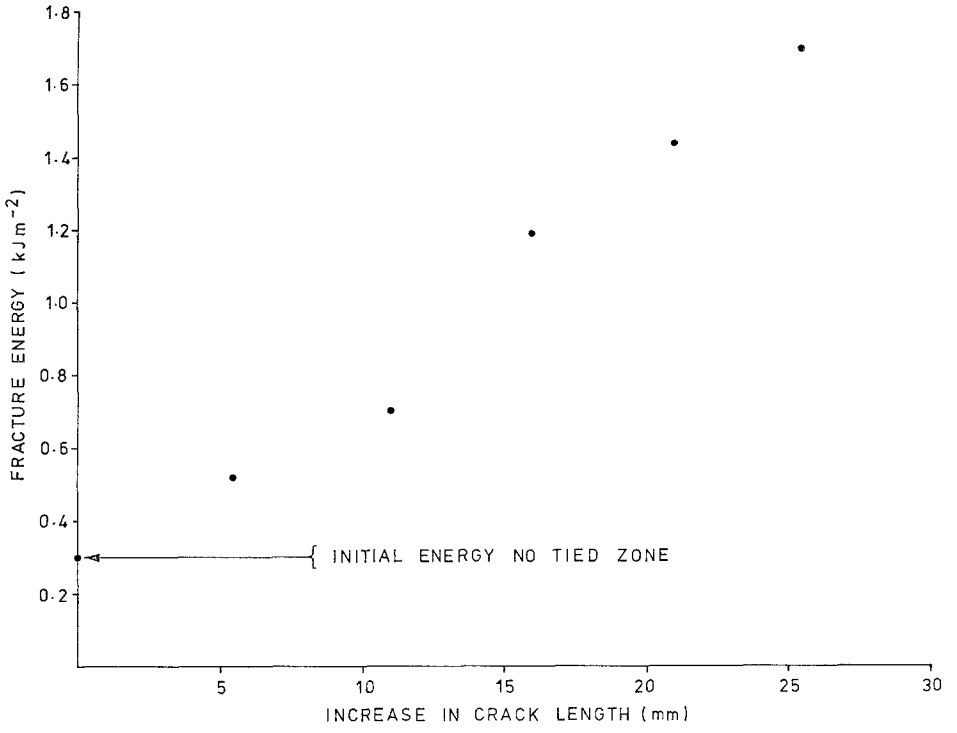

Figure 11 The increase in required fracture energy during crack growth.

TABLE V Mechanical properties of the composites, normalized to 60 vol%. Mean values are tabulated. Uncertainties are: strength 5% ; Young's modulus 3% ; interlaminar shear strength 3%

Composite	Composition	Strength (MN m^{-2})	Young's modulus (GN m^{-2})	Interlaminar shear strength (MN m^{-2})
C1	MY750/MNA/BDMA	1038	184	67
		1111	198	67
C2	MY750/piperidine	1068	196	71
		1102	193	70
C3	3.2% B	1104	185	72
		1114	188	72
C4	6.2% B	1044	192	65
		1039	193	64
C5	9.0% C	1086	186	67
		1049	191	69

Uncertainties are standard errors of the mean.

associated with the addition of the co-polymer systems.

4.3. Suppression of toughening

The obvious difference between the resin in a composite and the resin in bulk, is that in the former case it exists as a thin film, coating and joining the fibres. This film can be very thin, ranging from less than 1 μm to several μm. In order to examine whether the resin in thin film form possessed less toughness than in the bulk, the toughness of adhesive layers of the matrix systems were measured. These data were obtained by measuring the toughness of the bonds of adhesively joined aluminium cantilevers with a glue-line thickness of 0.2 mm, and are shown in Table VI. All failed almost totally cohesively, and only the cohesive failure data are

TABLE VI The initial fracture energies of the composites, and the fracture energies of the adhesive films and bulk resins

Resin system	Fracture energies (kJ m^{-2})		
	Bulk resin	Adhesive film*	Composite
MY750:MNA:BDMA	0.16 ± 0.01	0.14	0.24 ± 0.02
MY750:piperidine	0.33 ± 0.02	0.28	0.28 ± 0.03
MY750 + 3.2% B	1.40 ± 0.10	0.33	0.37 ± 0.03
MY750 + 6.2% B	2.20 ± 0.20	1.35	0.36 ± 0.04
MY750 + 9% C	3.20 ± 0.30	1.50	0.49 ± 0.07

*Uncertainties are ~ 10 to 20%.

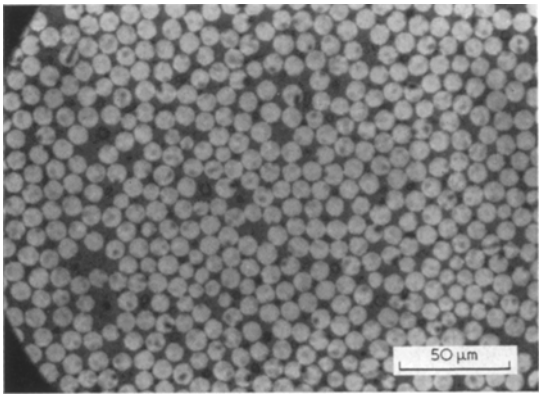

Figure 12 Microstructure of a composite with a rubber toughened matrix.

included in the table. Although the glue-line thickness at 200 µm is considerably greater than the resin film thickness in the composite, there has again been a suppression in toughness of the rubber toughened material compared with the bulk material. One adhesive bond was tested with a glue line thickness of 100 µm. This contained 9% polymer C and exhibited an energy of 1.18 kJ m^{-2} which, when compared with a 200 µm glue line toughness of 1.50 kJ m^{-2}, supports the trend of decreasing toughness with decreasing film thickness.

The mechanism by which the addition of a rubber precipitate toughens an epoxide resin is not well understood. At least three models can be hypothesized. These are:

Rubber particle tearing–rubber spheres which intersect the crack plane can elongate and tear as the fracture faces open;

Localized crazing – in rubber modified thermoplastics it has been shown that the toughening effect of the rubber results from the development of a great deal of crazing in the vicinity of the rubber spheres, under stress [11];

Plastic zone effects – a proportion of the co-polymer may remain in solution and by plasticizing the resin lead to a reduction in yield stress and a consequent increase in energy absorption due to plastic flow.

Of these, rubber particle tearing is an essentially local effect occurring only in the immediate vicinity of the crack plane and is, therefore, not likely to be affected by film thickness. The other two effects could occur over the volume associated with the crack tip stress field and, therefore, would be affected by film thickness. There is little evidence in the literature of crazing in cross-linked thermosetting materials such as epoxides. Consequently, to test the hypothesis of plasticization of the matrix by dissolved co-polymer, the yield stresses of the different, unreinforced resins were measured in compression. Fig. 13 shows a typical load versus compression curve of such a specimen. The yield stresses were calculated from the maximum loads on the basis of a 45° shear and were found to be reproducible to better than 1%. Table VII compares the values for the different systems. For the untoughened epoxides, of which the fracture energy might be expected to be controlled by a yielding mechanism, the fracture energy is smaller for the higher yield stress as would be qualitatively expected. For the toughened resins there is, however, little or no significant variation of yield stress although the toughnesses vary considerably. This strongly suggests that the increase in toughness by the addition of rubber is not due to plasticization.

McGarry [5] has attributed the rubber toughening of epoxides to a similar mechanism to that of rubber toughened thermoplastics, the generation of crazing in the vicinity of the inclusions. There is, however, very little evidence in the literature of crazing occurring in well-cured thermosets. Recently, Lilley and Holloway

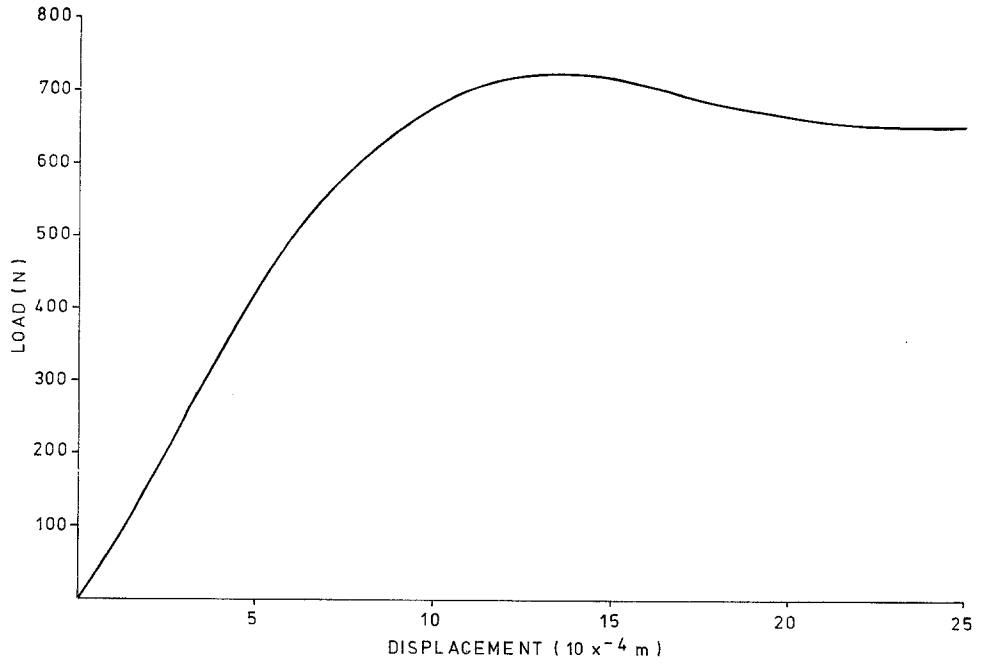

Figure 13 Compressive yielding of an epoxide.

TABLE VII The upper yield stresses and fracture energies of the resins

Resin system	Fracture energy (kJ m^{-2})	Yield stress (MN m^{-2})
MY750:MNA:BDMA	0.16	63
MY750:piperidine	0.33	45
MY750 + 3.2% B	1.40	43
MY750 + 6.2% B	2.20	43
MY750 + 9% C	3.20	41

[12] have published photographs of craze-like features in well-cured epoxides after stressing for considerable periods of time. Van den Boogart [13] has reported seeing crazes around crack tips in an incompletely cured resin system very similar to MY750. It is possible that the addition of rubber prevents complete cross-linking in the vicinity of rubber particles and thus permits crazing, and the rough fracture surfaces as shown in Fig. 8 may be caused by this effect. However, a detailed examination of this phenomenon has not been made in this work.

5. Conclusion

Considerable increases in the toughness of epoxide resins can be achieved by the addition of carboxyl terminated acrylonitrile-butadiene co-polymers, which cause the precipitation of a second phase. Addition of the co-polymers to the matrices of CFRP composites does not detract from their conventional properties such as flexural strength, modulus and interlaminar shear strength. The considerable increases in toughness obtained in the unreinforced resin are not translated into the composite, instead modest but significant increases are obtained for cracks propagating parallel to fibres. This effect is due to a suppression of the rubber toughening mechanism and is associated with resin film thickness. As a crack grows parallel to fibres, it develops a tied zone and the toughness increases to a value determined by processes characteristic of a fibre composite.

Acknowledgements

We are grateful to W. H. McCausland and P. Venables for their assistance in this work, and to P. R. Goggin for the measurement of single filament properties.

References

1. P. W. R. BEAUMONT and B. HARRIS, "Carbon Fibres – Their composites and applications", Proceedings of the International Conference organized by the Plastics Institute (1971) Paper No. 49.

2. G. R. SIDEY and F. J. BRADSHAW, *ibid* Paper No. 25.
3. P. W. R. BEAUMONT and D. C. PHILLIPS, *J. Composite Materials* **6** (1972) 32.
4. D. C. PHILLIPS, *ibid* **8** (1974) 130.
5. F. J. MCGARRY, *Proc. Roy. Soc. Lond* **A319** (1970) 59.
6. Information quoted in B. F. Goodrich Chemical Co. published literature on "Hycar" elastomers, based on work by F. J. McGarry and A. Willmer MIT R68-68, 1968.
7. N. L. HANCOX and H. WELLS, AERE-R7296 (1973).
8. J. V. LARSEN, 26th Annual Technical Conference, 1971, Reinforced Plastics/Composites Division, The Society of the Plastics Industry Inc. Paper No. 10-D.
9. M. HOCKNEY, private communication.
10. S. MOSTOVOY, P. B. CROSLEY and E. J. RIPLING, *J. Materials* **2** (1967) 661.
11. C. B. BUCKNALL and R. R. SMITH, *Polymer* **6** (1965) 437.
12. J. LILLEY and D. G. HOLLOWAY, *Phil. Mag.* **28** (1973) 215.
13. A. VAN DEN BOOGART, "The Physical Basis of Yield and Fracture", Institute of Physics Conference Proceedings **1** (1966) 167.

Received 21 October and accepted 8 November 1974.